Available online at www.sciencedirect.com
ScienceDirect
International Journal of Thermal Sciences 48 (2009) 1017–1025
International Journal of Thermal Sciences
www.elsevier.com/locate/ijts

Development and comparison of two-bed silica gel–water adsorption chillers driven by low-grade heat source

Z.Z. Xia *, R.Z. Wang, D.C. Wang, Y.L. Liu, J.Y. Wu, C.J. Chen

Institute of Refrigeration and Cryogenics, Shanghai Jiao Tong University, 800 Dongchuan Road, Shanghai 200240, China

Received 20 November 2007; received in revised form 30 June 2008; accepted 1 July 2008

Available online 3 August 2008

Abstract

A novel silica gel–water adsorption chiller (driven by hot water of 60–90 °C) with three vacuum chambers has been built in Shanghai Jiao Tong University (SJTU). This chiller was an improvement of an earlier deigned chiller and it integrated two single-bed systems (basic system) with only one vacuum valve. The performance of the chiller was tested and compared with the former adsorption chiller. The results show that the cooling power and COP of the chiller are 8.70 kW and 0.39 for the heat source temperature of 82.5 °C, cooling water temperature of 30.4 °C and chilled water outlet temperature of 12 °C. For a higher chilled water outlet temperature of about 16 °C, the COP increases to 0.43 while the cooling power is about 11.0 kW. Compared with that of the former chiller, the COP of this chiller increases by 20%.

Keywords: Adsorption; Silica gel; Refrigeration; Vacuum chamber; Chiller

1. Introduction

Adsorption refrigeration has attracted much attention in recent years because it can use environmentally friendly working fluids, such as ammonia, water, methanol, etc. Furthermore, adsorption systems can be powered by low grade heat source (e.g., waste heat from industrial processes or solar energy) and hence can contribute to energy savings. However, performance of adsorption refrigeration systems is poorer compared with that of conventional vapor compression systems. Many efforts have been made to improve the COP of adsorption refrigeration systems. Shelton [1] and Critoph [2] introduced two advanced adsorption cycles: the thermal wave cycle and convection thermal wave cycle, respectively. Pons [3], showed that a zeolite–water adsorption refrigeration system using the thermal wave cycle for air conditioning application had a 40–120 W kg^{-1} specific cooling power (SCP) and a COP of 0.3–0.4. From Sward's results [4], the cycle COP was higher than 1.2 for a thermal-wave adsorption heat pump cycle. Critoph [5,6] studied the convectional thermal wave cycle with a packed bed of inert materials such as steel ball, whereas, Wang [7] showed that 10–20% improvement of COP was obtained with a mass recovery process. In order to improve the system performance under a low temperature driving heat source, Saha et al. [8] proposed a four-bed and two-stage silica gel–water adsorption chiller, which utilized solar energy or a waste heat source of temperature between 40 and 75 °C. The COP and cooling power of this adsorption chiller was 0.36 and 3.2 kW, respectively when the hot water temperature and the cooling water temperature were 55 and 30 °C, respectively. Based on the four-bed and two-stage adsorption chiller, a six-bed silica gel–water adsorption chiller was developed by Saha and his coworkers [9]. This adsorption chiller was operated under two modes: the single-stage mode and the three-stage mode. The single-staged mode was adopted for a heat source temperature ranging from 60 to 90 °C, whereas the other mode was employed when the heat source temperature was between 40 and 60 °C.

In this paper, an improved silica gel–water adsorption chiller has been designed and built, based on our earlier work [10]. In this improved chiller, one condenser, one adsorber and one evaporator were housed in one vacuum chamber to form an adsorption/desorption unit. The experimental results of the improved adsorption chiller are given in this paper. Also, a comparison of the performance of the former adsorption chiller and the improved one is presented.

* Corresponding author. Tel.: +86 21 34206296; fax: +86 21 34206296.
E-mail address: xzz@sjtu.edu.cn (Z.Z. Xia).

1290-0729/$ – see front matter
doi:10.1016/j.ijthermalsci.2008.07.004

Nomenclature

C_{cu}	specific heat capacity of copper	$kJ\,kg^{-1}\,K^{-1}$	
$C_{p,w}$	specific heat capacity of water	$kJ\,kg^{-1}\,K^{-1}$	
COP	coefficient of performance		
ΔT_e	temperature difference of the evaporator	K	
ΔT_{me}	temperature difference of the methanol evaporator	K	
$\dot{G}_{chilled}$	flow rate of chilled water	$kg\,s^{-1}$	
$\dot{G}_h$	flow rate of hot water	$kg\,s^{-1}$	
L_{meth}	latent heat of methanol	$kJ\,kg^{-1}$	
m_e	mass of water evaporator metal	kg	
m_{me}	mass of methanol evaporator metal	kg	
$m_{meth,residual}$	mass of residual methanol	kg	
$m_{c,w}$	mass of water in water evaporator	kg	
n	times of data acquisition in one cycle		
Q_{ref}	cooling power	kW	
Q_h	heating power	kW	
$Q_{loss,imp}$	cooling power loss	kW	
SCP	specific cooling power	$W\,kg^{-1}$	
$T_{chilled,in}$	inlet temperature of chilled water	°C	
$T_{chilled,out}$	outlet temperature of chilled water	°C	
$T_{h,in}$	inlet temperature of hot water	°C	
$T_{h,out}$	outlet temperature of hot water	°C	
τ_{cycle}	cycle time	s	

Superscript

i	the order number of the data acquisition interval

2. System description

Fig. 1 shows the photograph of the improved silica gel–water adsorption chiller and the former chiller. The heat source/heat sink switching system of the improved chiller consists of 11 electric valves and connecting pipes. The electric valves are all controlled by a PLC in the control box. The novel adsorption chiller with a dimensions of 1.8 m × 1.5 m × 0.92 m is composed of three chambers: two vacuum chambers and one methanol evaporator (shown in Fig. 2), whereas the former chiller with a dimensions of 0.8 m × 0.7 m × 0.95 m consists of only two vacuum chambers. Each of the vacuum chambers contains one evaporator, one condenser and one adsorber. Water is used as the refrigerant in the two vacuum chambers. In the improved chiller, a vacuum valve is installed between the two vacuum chambers to carry out the mass recovery process. The improved adsorption chiller integrates two water evaporators with one methanol evaporator to form a gravitation heat pipe loop, in which methanol is used as the working substance. The cooling power is transferred from one water evaporator into the methanol evaporator via the gravitation heat pipe loop and finally taken away by the chilled water passing through the methanol evaporator.

As is shown in Fig. 3(a), the improved adsorption chiller has six operating processes: two adsorption/desorption processes, two mass recovery processes and two heat recovery processes. Fig. 3(b) shows the Clapeyron diagram for the cyclic processes of the chiller. For the purposes of describing the cycle, it is assumed that the cyclic process starts when the adsorber 1 and the adsorber 2 are in the desorption and adsorption processes respectively. The six processes presented in Fig. 3 are described as follows:

2.1. *Adsorber 1 is in desorption process and adsorber 2 is in adsorption process (adsorber 1:* B → n → C*, adsorber 2:* E → m → F*)*

Hot water is used to heat adsorber 1, which desorbs the refrigerant (water), while cooling water is used to cool condenser 1, condenser 2 and adsorber 2 in sequence. The desorbed water vapor condenses in evaporator 1 initially since temperature of evaporator 1 is lower than that of condenser 1. The

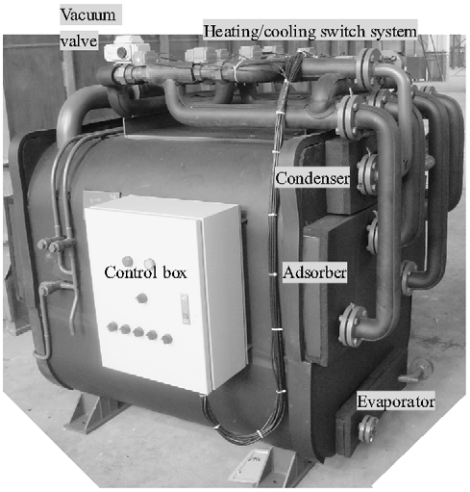

(a)

(b)

Fig. 1. Photograph of the improved adsorption chiller and the former adsorption chiller. (a) The improved adsorption chiller. (b) The former adsorption chiller [10].

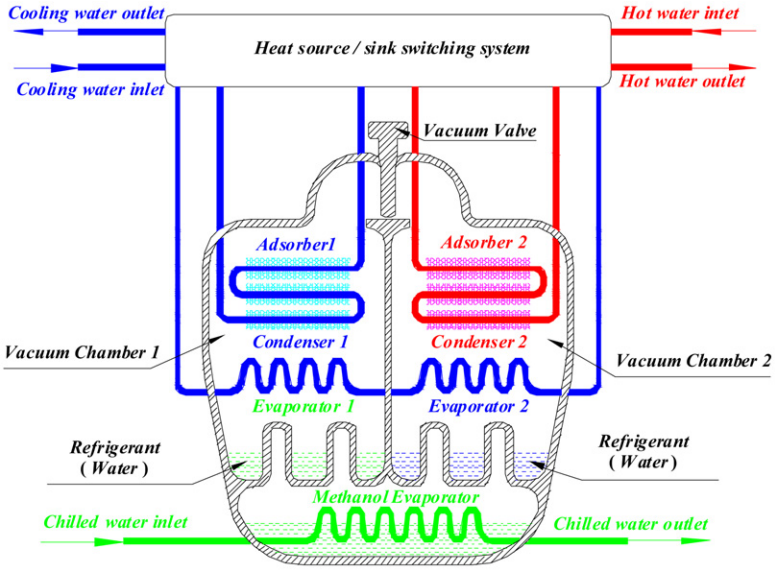

Fig. 2. Schematic diagram of the improved adsorption chiller.

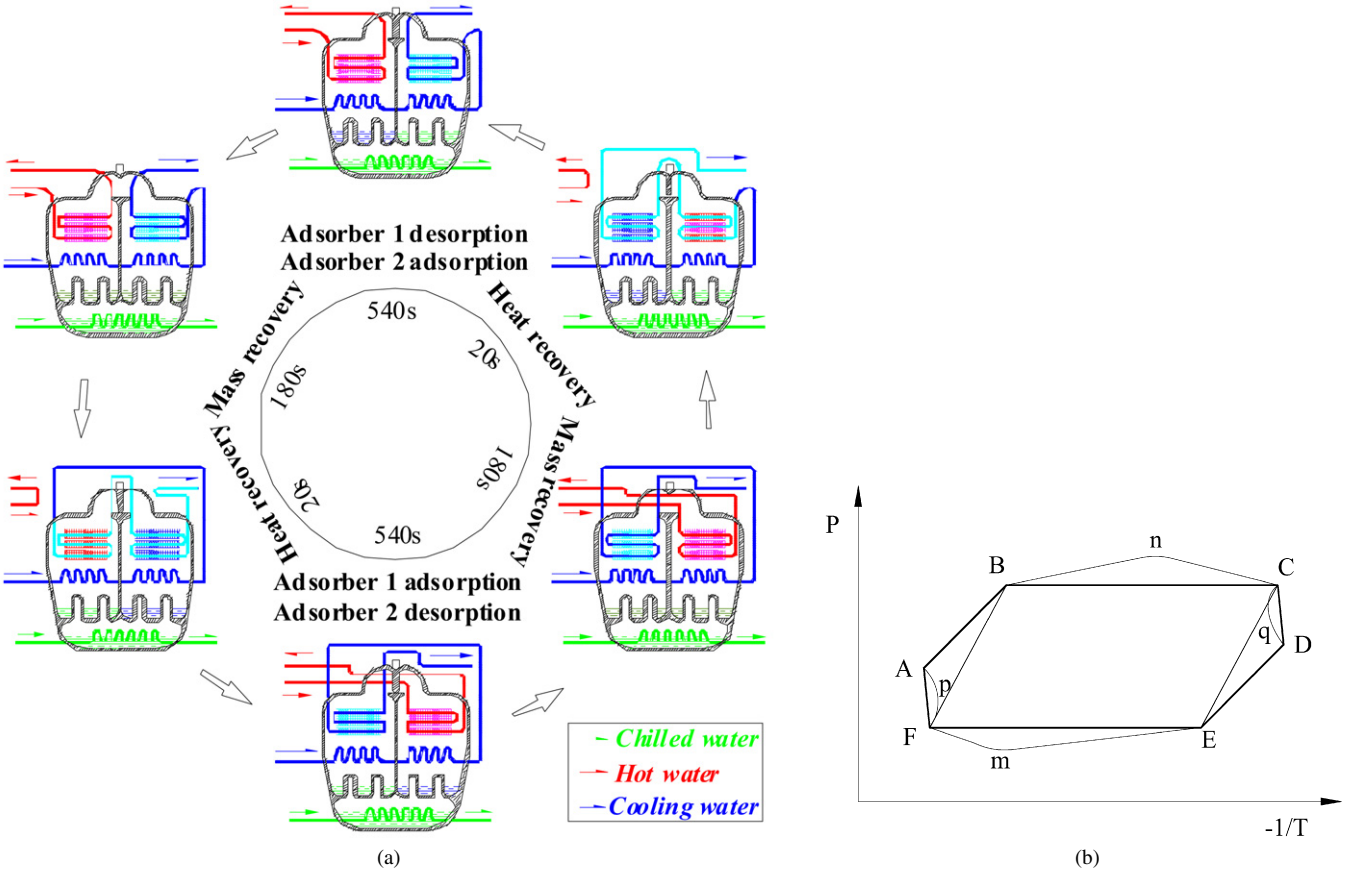

Fig. 3. The cyclic process of the improved adsorption chiller. (a) Schematic diagram of cyclic process. (b) Claperyon diagram of the cyclic process.

condensation takes place in condenser 1 when the pressure in vacuum chamber 1 is higher than the saturation pressure of condenser 1. Then the condensate flows back to evaporator 1. At the same time, adsorber 2 is cooled and adsorbs water from evaporator 2. So the temperature of evaporator 2 decreases due to the evaporation of water. The methanol in the methanol evaporator evaporates when the temperature of the methanol vapor is lower than the temperature of the evaporator 2. Thus the chilled water is cooled when it flows through the heat exchange tubes in the methanol evaporator. Since the temperature of evaporator 1 is higher than those of evaporator 2 and the methanol evaporator, heat is only transferred from methanol evaporator to evapora-

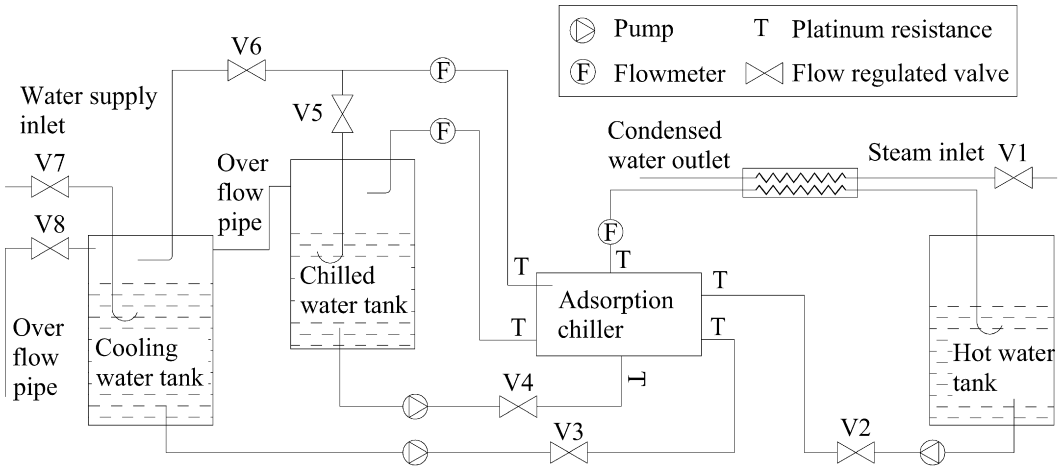

Fig. 4. Schematic diagram of the testing system of the silica gel–water adsorption chiller.

tor 2 according to the working principle of gravitation heat pipe loop.

2.2. Mass recovery from adsorber 1 to adsorber 2 (adsorber 1: C → q → D, adsorber 2: F → p → A)

After the first process, the vacuum valve is opened. Since the pressure in vacuum chamber 1 is much higher than that of vacuum chamber 2, the water vapor flows into vacuum chamber 2. During this process, adsorber 1 is still heated by the hot water while adsorber 2 is cooled by the cooling water. As a result, adsorber 1 continues desorbing the refrigerant and adsorber 2 keeps adsorbing refrigerant. So the cycled refrigerant mass is greatly improved.

2.3. Heat recovery from adsorber 1 to adsorber 2 (adsorber 1: D → E, adsorber 2: A → B)

The mass recovery process finishes when the pressures of the two vacuum chambers are almost in equilibrium. The hot water is bypassed while the cooling water flows into the adsorber 1. Then the residual hot water in the adsorber 1 was forced into adsorber 2 by the cooling water, thus heat is recovered. During this process, adsorber 1 is cooled by cooling water and the adsorber 2 is heated by the residual hot water coming from adsorber 1.

2.4. Adsorber 1 is in adsorption stage and adsorber 2 is desorption stage (adsorber 1: E → m → F, adsorber 2: B → n → C)

In this process, adsorber 1 is cooled in order to adsorb the refrigerant from evaporator 1 while adsorber 2 desorbs refrigerant into condenser 2. Meanwhile, evaporator 2 and condenser 1 become idle.

2.5. Mass recovery from adsorber 2 to adsorber 1 (adsorber 1: F → p → A, adsorber 2: C → q → D)

When the adsorbers stop adsorbing or desorbing, the vacuum valve is opened for the mass recovery process, which is similar to the second process. During this process, adsorber 2 is heated by hot water while adsorber 1 is cooled by the cooling water.

2.6. Heat recovery from adsorber 2 to adsorber 1 (adsorber 1: A → B, adsorber 2: D → E)

In this process, the residual hot water in adsorber 2 is forced into adsorber 1 by the cooling water. As a result, adsorber 2 is cooled while adsorber 1 is heated by the residual hot water. After this process, a new cycle begins.

Although one evaporator and one condenser are idle during the whole cycle, which decreases the utilization ratio of the evaporators and the condensers, the vacuum valves, which are necessary for conventional adsorption refrigeration systems, could be reduced to one for mass recovery. It is well known that at least four vacuum valves are necessary in a conventional adsorption refrigeration system in order to carry out a continuous cooling power output. Since the vacuum valves are quite expansive and relatively unreliable, the reliability and economics of the improved adsorption chiller are improved significantly, compared with a conventional adsorption refrigeration system.

3. Testing system

Fig. 4 shows the schematic diagram of the testing system of the improved adsorption chiller. Three water supply systems were adopted: the hot water, the cooling water and the chilled water systems. One flowmeter was installed in each water supply system. Valves V2, V3 and V4 were used to control the water flow rate. The heat source was provided by a shell and tube heat exchanger which was heated by steam flow at a pressure of 600 kPa. Hot water temperature was controlled using valve V1. The chilled water and cooling water temperatures were controlled by valves V5 and V7, respectively, and

Table 1
Comparisons of performance of the improved chiller and the former chiller

Prototype	Hot water temp. (°C)	Cooling water temp. (°C)	Chilled water temp. (°C)		Refrigerating capacity (kW)	COP	SCP (W/kg)	Cycle time (s)
			Inlet	Outlet				
The improved chiller	78.8	31.3	20.5	16.0	8.32	0.31	80.0	1680
	81.8	31.3	20.7	16.3	9.33	0.34	89.7	1920
	86.8	30.9	21.1	16.3	10.62	0.40	102.1	1920
	59.7	30.4	20.5	18.2	4.80	0.39	46.2	2280
	69.1	30.3	19.6	16.2	7.57	0.38	72.8	
	84.4	30.5	21.5	16.5	10.88	0.43	104.6	
	85.3	30.6	20.9	16.1	10.44	0.40	100.4	
	80.3	30.2	15.8	12.1	8.26	0.38	79.4	
	82.5	30.4	15.8	11.9	8.69	0.39	83.6	
	83.8	30.8	15.4	11.8	8.61	0.38	82.7	
The former chiller in Ref. [10]	85	32	14	–	–	0.313*[1]	–	1000
	85	30	14	–	–	0.361*[1]	–	
	85	32	14	13	2.27	0.188*[2]	43.0	
	85	30	14	12.8	2.79	0.212*[2]	52.8	

Note: *[1] Based on the *second prototype* studied in Ref. [10];
*[2] Based on the *first prototype* studied in Ref. [10].

valves V6 and V8 acted as assistant controllers. Compared with the cooling water tank, the chilled water tank was located at a higher position so that the superfluous chilled water can flow into the cooling water tank via an over-flow pipe. Furthermore, the cooling water was discharged by another over-flow pipe. The cooling power and heating power were calculated as follows:

Cooling power:

$$Q_{\text{ref}} = \sum_{i=1}^{n} \left[\dot{G}_{\text{chilled}} \cdot C_{p,w} \cdot \left(T^{i}_{\text{chilled,in}} - T^{i}_{\text{chilled,out}} \right) \right] / n \qquad (1)$$

where $\dot{G}_{\text{chilled}}$ (kg s^{-1}) is the flow rate of the chilled water, $C_{p,w}$ (kJ kg^{-1} K^{-1}) is specific heat capacity of water, $T_{\text{chilled,in}}$ (°C) and $T_{\text{chilled,out}}$ (°C) are the inlet and outlet temperature of the chilled water, respectively, superscript word 'i' is the order number of the data acquisition interval, and n is the frequency of data acquisition in one cycle.

Heating power:

$$Q_h = \sum_{i=1}^{n} \left[\dot{G}_h \cdot C_{p,w} \cdot \left(T^{i}_{h,\text{in}} - T^{i}_{h,\text{out}} \right) \right] / n \qquad (2)$$

where $\dot{G}_h$ (kg s^{-1}) is the flow rate of the hot water, and $T_{h,\text{in}}$ (°C) and $T_{h,\text{out}}$ (°C) are the inlet and outlet temperature of the chilled water, respectively.

Then the COP is expressed as:

$$\text{COP} = \frac{Q_{\text{ref}}}{Q_h} \qquad (3)$$

Each operating condition shown in this paper was repeated several cycles until stable temperature profiles of this improved chiller were obtained. The data were acquired by a Keithly 2700 Multimeter/Data Acquisition System every 9 seconds. The water inlet and outlet temperatures of the chiller were measured by six PT100 platinum resistors with precisions of ±0.15 and ±0.10 °C. The maximum uncertainties of the hot water inlet and outlet temperature difference, the cooling water inlet and outlet temperature difference and the chilled water inlet and outlet temperature difference were 0.30, 0.30 and 0.20 °C, respectively. The water flow rates were measured using three flow meters with 1% FS (full scale) accuracy. So the relative error for cooling power ranged from 4.4 to 8.8% under the given operating conditions. And the relative error for COP was between 8.0 and 14.9%. The total mass of silica gel adopted in the improved chiller is 104.0 ± 0.2 kg. As a result, the relative error for SCP varied from 4.4 to 8.8%.

4. Results and discussions

4.1. Comparisons of experimental results

Table 1 shows the performance comparisons of the improved adsorption chiller and the former chiller. Since most of the experimental results of the former chiller were obtained under 28 °C cooling water temperature in Ref. [10], Table 1 only shows the experimental results based on the similar testing conditions.

The cooling power of the improved chiller reached 10.9 kW with a SCP of 104.6 W/kg when the cooling water temperature, hot water temperature and chilled water outlet temperature were 30.6, 84.4 and 16.5 °C, respectively. Furthermore, a cooling power of 4.80 kW was obtained when the hot water temperature was about 60 °C and the cooling water temperature was 30.4 °C, though the chilled water outlet temperature was a bit higher, about 18.2 °C. This result indicates that a good performance for the improved chiller working under a low-grade heat source can be obtained, which is impossible for the former chiller.

When the chilled water outlet temperature was 15.4 °C, a COP and cooling power of 0.38 and 8.61 kW, respectively, were gotten. Compared with the first prototype of the former chiller, a 57 and 80.7% improvement in the SCP and COP, respectively, can be obtained even though the hot water temperature in the present study was 1.2 °C lower than that of the typi-

Table 2
Performance of the chiller with mass recovery process

Prototype	Mass recovery time (s)	Hot water temp. (°C)	Cooling water temp. (°C)	Chilled water temp. or evaporating temp. (°C)		Refrigerating power (kW)	COP	Desorption time (s)
				Inlet	Outlet			
The improved chiller	60	84.1	30.6	20.6	16.2	8.87	0.43	900
	90	83.9	30.2	20.5	15.9	9.41	0.45	
	120	84.7	30.3	20.5	15.9	9.54	0.43	
	150	84.2	30.5	20.7	16.1	9.29	0.41	
	180	84.3	30.5	20.6	16.1	9.39	0.43	
	210	84.6	30.5	20.7	16.2	9.23	0.43	
	90	84.8	30.9	20.5	16.2	8.70	0.41	840
	120	84.9	31	20.8	16.5	8.84	0.41	
	150	85.1	31.1	20.8	16.4	8.94	0.42	
	180	84.9	31	20.8	16.4	9.00	0.42	
	210	84.9	30.8	20.7	16.2	9.22	0.41	
The former chiller in Ref. [10]	0	85	28	10		3.05	0.208*[2]	480
	20					3.56	0.276*[2]	
	60					3.70	0.240*[2]	
	100					3.23	0.220*[2]	

Note: *[2] Based on the *first prototype* studied in Ref. [10].

cal condition in Ref. [10]. Compared with the second prototype of the former chiller, the improvement in the COP was about 20%. Under a similar working condition with 12 °C chilled water outlet temperature, the SCP of the improved chiller increased by more than 90%.

4.2. Influence of mass recovery process on the adsorption chiller

The performance of the improved and the former adsorption chillers with mass recovery process is shown in Table 2. When the desorption time was kept constant, the COP of the improved adsorption chiller changed a little with the increase of the mass recovery time. However, when desorption time was decreased from 900 to 840 s, the maximum difference of COP was about 0.05, which was almost 10% of the original COP value. The cooling power initially increased with the increase of the mass recovery time when the desorption time was about 900 s; however, it decreased when the mass recovery time was larger than 120 s. But for the 840 s desorption time, the cooling power output increased continuously with the increasing mass recovery time.

Compared with a basic adsorption refrigeration cycle, the mass recovery process will greatly improve the cycled refrigerant mass (shown in Fig. 3(b)). Since the desorber desorbs more refrigerant in a mass recovery cycle compared with a cycle without mass recovery process, the desorber will adsorb more refrigerant from the evaporator in the next adsorption process, which results in a larger cooling power output. With the increase of mass recovery time, the cycled refrigerant mass will increase sharply at first, and then the increasing rate becomes smaller. Since no cooling power yields during the mass recovery process, with the increase of mass recovery time, the cooling power increases firstly and then decreases due to the decrease of the increasing rate of the cycle refrigerant mass during the mass recovery process. As a result, an optimized mass recovery time should be chosen in order to get a maximum cooling power output. Therefore, if the desorption time is long enough, a short mass recovery time should be adopted. Whereas, if a short desorption time is chosen, a long mass recovery time is necessary to improve the performance.

Table 3
Performance of the improved chiller under different cooling water and hot water temperatures

Hot water temp. (°C)	Cooling water temp. (°C)	Chilled water (°C)		Refrigerating power (kW)	COP
		Inlet	Outlet		
85.3	30.6	20.9	16.1	10.44	0.40
80.8	30.9	20.8	16.0	10.09	0.42
74.8	30.5	20.7	16.8	8.76	0.42
69.1	30.3	19.6	16.2	7.57	0.38
65.3	30.5	20.5	17.6	6.66	0.34
85.4	30.3	15.5	11.7	8.23	0.37
80.3	30.2	15.8	12.1	8.26	0.38
75	30.9	15.7	12.9	6.52	0.36

The expected mass recovery time for the improved adsorption chiller varies from 90 to 180 s under a different desorption time. The COP and the cooling power of the former adsorption chiller increase by 32.7 and 16.7% for the mass recovery time of 20 s.

4.3. Influence of chilled water temperature and hot water temperature

Experimental and practical investigations in Europe have proved that closed cyclic chilled-ceilings can remove high cooling loads with consideration of human thermal comfort. In order to avoid discomfort caused by asymmetric radiant temperature, the surface temperature of the ceiling panels should be ranged from 18 to 22 °C during cooling (as recommended by ISO 7730 [11]). As a result, the evaporating temperature of the chiller could be larger than 15 °C. As shown in Table 3, the cooling power and COP were about 10.44 and 0.40 kW when

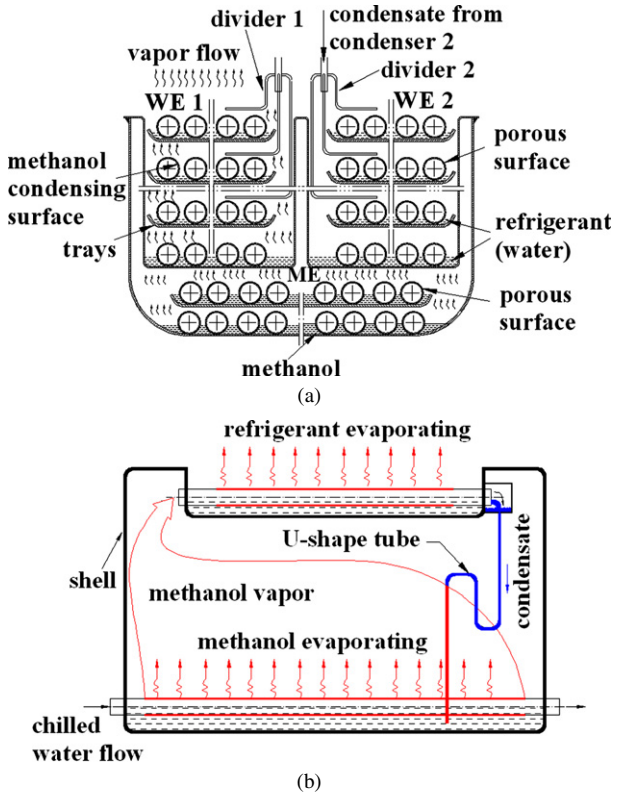

Fig. 5. Evaporators integrated with heat pipe technique in the improved chiller. (a) Heat-pipe combined evaporator. (b) Gravitation heat pipe loop.

the temperature of hot water, temperature of cooling water and inlet temperature of chilled water were about 85.3, 30.6 and 20.9 °C, respectively. Thus the improved adsorption chiller is highly efficient for air conditioning without dehumidification. However, when the inlet chilled water was about 15.5 °C, the cooling power and COP decreased by 21 and 9%, respectively. The influence of hot water temperature on the performance of the improved adsorption chiller is also presented in Table 3. The cooling power varied from 6.66 to 10.44 kW when the hot water temperature increased from 65.3 to 85.3 °C.

The improved adsorption chiller can be used for an air conditioning system with a low dehumidified load. And a good economic return will be expected. In fact, the improved adsorption chiller has already been applied in a green building, low-temperature grain storage and a novel micro-scale combined cooling, heating and power (MCCHP) system [12–15].

4.4. Effects of the improvement in the structure of the evaporator

4.4.1. The cooling power losses in the evaporators

Fig. 5 shows the evaporators integrated with heat pipe technique in the improved adsorption chiller. The methanol evaporator acts as the evaporation section of the heat pipe loop, whereas the water evaporator is the condensation section of the heat pipe loop. Methanol evaporates on the external surface of the tube in the methanol evaporator when the chilled water flows through the tube. The methanol vapor is then cooled by the evaporation of the refrigerant in one of the water evaporator (for example, evaporator 1) and condenses on the internal surface of the copper tube in the water evaporator. Finally the condensate of the methanol flows down to the methanol evaporator on a U-shaped channel. As a result, the chilled water flowing through the internal surface of the tube in the methanol evaporator is cooled. At the same time, the other water evaporator (for example, evaporator 2) collects the refrigerant condensate coming from the condenser in the same vacuum chamber.

However after the adsorption process of adsorber 1, some methanol condensate remains in the bottom of the tubes in the evaporator 1 due to the horizontal arrangement of these tubes. When the desorption process of the adsorber 1 starts, the residual methanol condensate evaporates and condenses in the evaporator 2 or the methanol evaporator. In this process, the methanol vapor from evaporator 1 is cooled by the evaporation of the refrigerant in evaporator 2. Thus the cooling power loss occurs. Moreover, the condensation of refrigerant in vacuum chamber 1 initially takes place in the evaporator 1 because the temperature of evaporator 1 is smaller than that of the condenser 1. And this also causes a cooling power loss. As a result, this cooling power loss can be evaluated in terms of the mass of the evaporator metal, the mass of water in the water evaporator and the residual methanol.

$$m_{\mathrm{meth,residual}} \approx \frac{m_e C_{\mathrm{cu}} \Delta T_e + m_{\mathrm{me}} C_{\mathrm{cu}} \Delta T_{\mathrm{me}}}{L_{\mathrm{meth}}} = \frac{65 \times 0.386 \times 20 + 28 \times 0.386 \times 6}{1250} = 0.45\ \mathrm{kg} \tag{4}$$

$$Q_{\mathrm{loss,jmp}} = \frac{m_e C_{\mathrm{cu}} \Delta T_e + m_w C_{p,w} \Delta T_e + L_{\mathrm{meth}} m_{\mathrm{meth,residual}}}{\tau_{\mathrm{cycle}}/2} = \frac{65 \times 0.386 \times 20 + 5 \times 4.186 \times 20 + 28 \times 0.386 \times 6}{19 \times 60} = 0.98\ \mathrm{kW} \tag{5}$$

where the mass of residual methanol, $m_{\mathrm{meth,residual}}$, is determined by the physical property of the methanol, the structure of the water evaporator, the surface behavior of the water evaporator and the temperatures of the methanol and the methanol evaporator. So it is difficult to get an accurate value of $m_{\mathrm{meth,residual}}$. A conservative value was estimated on the basis of the temperature drop in the water evaporator and the temperature lift of the methanol evaporator obtained from the experimental results, as expressed by Eq. (4). The temperature difference of the evaporator, ΔT_e, is based on the evaporator temperature changing from 35 °C at the end of the desorption/condensation process to 15 °C at the end of the adsorption/evaporation process. ΔT_{me} is the temperature lift of the methanol evaporator caused by the condensation of the residual methanol vapor in the methanol evaporator. m_w is mass of water in the water evaporator after the adsorption process, which was 5.0 and 15.0 kg for the improved chiller and the former one respectively according the experimental result.

For the evaporator of the former chiller, the cooling power loss was mainly determined by the heat capacity of the evaporator material and the heat capacity of the chilled water residual

in the evaporator [10], and can be estimated by the following equation (6).

$$Q_{\text{loss,jmp}} = \frac{m_e C_{\text{cu}} \Delta T_e + m_w C_{p,w} \Delta T_e}{\tau_{\text{cycle}}/2} = \frac{32 \times 0.386 \times 20 + 15 \times 4.186 \times 20}{460} = 2.37 \text{ kW} \quad (6)$$

According to the evaluation above, the improvement in the structure of the evaporator was significant. The refrigeration loss in the evaporator was about 47.4% of the nominal cooling power of the former chiller and 9.85% for the improved chiller.

4.4.2. Heat transfer performance of the evaporators

According to Y.L. Liu et al. [10], the evaporators of the former chiller were plate and fin heat exchangers. Five sheets of 200-mesh wire gauze were attached to the wall of the refrigerant vapor channel. Due to the capillary force on the wire gauze, the water in the evaporator formed a thin liquid film on the wall of the heat exchanger during the adsorption process, which enhanced the evaporation of the water. However, since the height of the heat exchanger was about 100 mm, it was difficult to form a thin liquid film in the upper side of the heat exchanger.

In order to solve the above mentioned problem, a capillary assisted evaporation was introduced in the evaporators of the improved chiller. Heat exchanger tubes with porous surface were arranged on the trays (shown in Fig. 5). These heat exchanger tubes were immersed partly in the water, which was collected by the trays. The water liquid could flow upwards along the porous surface of the tubes by capillary suction and thus most of outer surface of the tube would be covered by a thin liquid film. As a result, the evaporation coefficient was greatly enhanced due to the extremely thin liquid film. Experimental result showed that, for water, the film side evaporation heat transfer coefficients were 3100–3500 $\text{W m}^{-2}\text{ K}^{-1}$ under the evaporation saturated temperature of $5.0 \pm 0.1\,^{\circ}\text{C}$ and superheating of $4.0 \pm 0.1\,^{\circ}\text{C}$ [16].

In addition, the variations of the evaporator temperature indicated that the evaporator of the improved chiller was effective. The comparisons of the temperature difference between the chilled water outlet and the evaporation temperature of the two chillers during adsorption process in half cycle are shown in Fig. 6. The time-averaged temperature difference between the evaporator temperature and the chilled water outlet temperature was about 2.4 °C, which was about 0.7 °C lower than that in Ref. [10]. So the decrease of this difference means an improvement in the potential cooling power of the chiller.

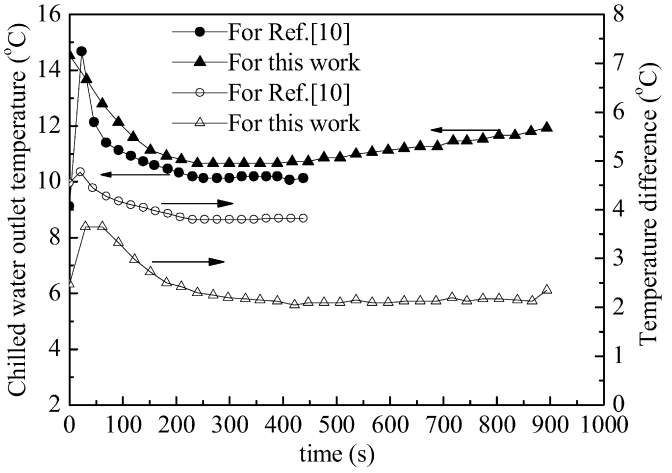

Fig. 6. Comparisons of the temperature difference between the chilled water outlet and the evaporating temperature of the two chillers.

5. Conclusions

An improved adsorption chiller with three vacuum chambers was designed, built and its performance was tested and compared with a former chiller. The following conclusions are made:

(1) The cooling power and COP of the chiller are 8.70 and 0.39 kW, respectively, for a heat source at 82.5 °C, the cooling water temperature at 30.4 °C and the chilled water outlet temperature at 12 °C.
(2) For a chilled water outlet temperature of about 16 °C, the COP increases to 0.43 while the cooling power is about 11.0 kW. There is an improvement of about 20% in COP, compared with the former chiller.
(3) The mass recovery process for the chiller yields a maximum improvement of 65% in the cooling power and about 32% in the COP. The mass recovery process has a larger influence on the cooling power, which is quite different from the mass recovery-like effects adopted in the former adsorption chiller.
(4) The evaporators used in the improved adsorption chiller are simpler, more efficient and more reliable compared with that of the former chiller.

Acknowledgements

This work was supported by the national 863 Program (HI-TECH RESEARCH AND DEVELOPMENT PROGRAM OF CHINA) under the contract No. 2006AA05Z413.

References

[1] S.V. Shelton, W.J. Wepfer, D.J. Miles, Ramp wave analysis of the solid/vapor heat pump, J. Energ. Resour. ASME 112 (1990) 69–78.
[2] R.E. Critoph, Forced convection enhancement of adsorption cycles, Heat Recovery Systems & CHP 14 (1994) 343–350.
[3] M. Pons, S. Szarzynski, An adsorption cooling system with heat-regeneration: experiment and numerical study, in: Progress of the International Sorption Heat Pump Conference, Munich, Germany, March 24–26, 1999, pp. 625–630.
[4] B.K. Sward, D. LeVan, F. Meunier, Adsorption heat pump modeling: the thermal wave process with local equilibrium, Appl. Therm. Eng. 20 (2000) 759–780.
[5] R.E. Critoph, Forced convection adsorption cycle with packed bed heat regeneration, Int. J. Refrig. 22 (1999) 38–46.
[6] R.E. Critoph, Forced convection adsorption cycles, Appl. Therm. Eng. 18 (1998) 799–807.
[7] R.Z. Wang, Performance improvement of adsorption heat pump by heat and mass recovery operation, Int. J. Refrig. 24 (2001) 602–611.

[8] B.B. Saha, A. Akisawa, T. Kashiwagi, Solar/waste heat driven two-stage adsorption chiller: the prototype, Renew Energy 23 (2001) 93–101.
[9] B.B. Saha, S. Koyama, T. Kashiwagi, A. Akisawa, K.C. Ng, H.T. Chua, Waste heat driven dual-mode, multi-stage, multi-bed regenerative adsorption system, Int. J. Refrig. 26 (2003) 749–757.
[10] Y.L. Liu, R.Z. Wang, Z.Z. Xia, Experimental study on a continuous adsorption water chiller with novel design, Int. J. Refrig. 12 (2005) 128–135.
[11] International Standard ISO 7730, Moderated Thermal Environments-Determination of PMV and PPD indices and Specification of the Conditions for Thermal Comfort, Ref. No. 7730, 1984(E) (August 1984).
[12] Q. Ma, R.Z. Wang, Y.J. Dai, X.Q. Zai, Performance analysis on a hybrid air-conditioning system of a green building, Energy Buildings 38 (2006) 447–453.
[13] X.Q. Zai, R.Z. Wang, Y.J. Dai, J.Y. Wu, Y.X. Xu, Q. Ma, Solar integrated energy system for a green building, Energy Building 39 (2007) 985–993.
[14] H.L. Luo, R.Z. Wang, Y.J. Dai, J.Y. Wu, J.M. Shen, B.B. Zhang, An efficient solar-powered adsorption chiller and its application in low-temperature grain storage, Sol. Energy 81 (2007) 607–613.
[15] Y. Huangfu, J.Y. Wu, R.Z. Wang, X.Q. Kong, B.H. Wei, Evaluation and analysis of a novel micro-scale combined cooling, heating and power (MCCHP) system, Energ. Convers. Manage. 48 (2007) 1703–1709.
[16] Z.Z. Xia, G.Z. Yang, R.Z. Wang, Experimental investigation of capillary-assisted evaporation on the outside surface of horizontal tubes, Int. J. Heat Mass Tran. 51 (2008) 4047–4054.